Ultrasound-Propelled Nanoporous Gold Wire for Efficient Drug Loading and Release

*Victor Garcia-Gradilla, Sirilak Sattayasamitsathit, Fernando Soto, Filiz Kuralay, Ceren Yardımcı, Devan Wiitala, Michael Galarnyk, and Joseph Wang**

Ultrasound (US)-powered nanowire motors based on nanoporous gold segment are developed for increasing the drug loading capacity. The new highly porous nanomotors are characterized with a tunable pore size, high surface area, and high capacity for the drug payload. These nanowire motors are prepared by template membrane deposition of a silver-gold alloy segment followed by dealloying the silver component. The drug doxorubicin (DOX) is loaded within the nanopores via electrostatic interactions with an anionic polymeric coating. The nanoporous gold structure also facilitates the near-infrared (NIR) light controlled release of the drug through photothermal effects. Ultrasound-driven transport of the loaded drug toward cancer cells followed by NIR-light triggered release is illustrated. The incorporation of the nanoporous gold segment leads to a nearly 20-fold increase in the active surface area compared to common gold nanowire motors. It is envisioned that such US-powered nanomotors could provide a new approach to rapidly and efficiently deliver large therapeutic payloads in a target-specific manner.

1. Introduction

The ability of synthetic nanomotors to transport therapeutic payloads to previously inaccessible areas of the body has been recognized as one of the next prospects for nanomotor development.[1–6] Future drug delivery nanovehicles, incorporating propulsion and navigation capabilities, should thus facilitate targeted and guided delivery of therapeutic loads to predetermined locations in the body. Progress in utilizing microscale motors for directed drug delivery has advanced rapidly in recent years.[1,7–12] Wang's team demonstrated the first proof-of-concept of directed delivery of common liposomal and polymeric drug carriers using chemically-powered catalytic nanowire motors.[7] Bubble-propelled nanomotors based on hydrogen peroxide fuel and release of DOX have been reported.[8] Unlike earlier use of chemically-powered nanomotors, externally-actuated (fuel-free) nanoshuttles are essential for future in vivo biomedical transport and drug delivery applications.[6,9–12] Recent efforts in this direction have focused on magnetically-actuated microswimmers as robotic drug delivery platforms.[9–11] The functionalization of such magnetically-actuated helical micromotors with drug-loaded temperature-sensitive liposomes has been described by Nelson's group.[12]

This article describes the use of ultrasound-powered highly-porous motors with large surface area and a high drug loading capacity. Ultrasound has found extensive applications in medicine, and holds considerable promise for driving micromotors in biological fluids.[6] The gold nanowire motors are propelled by ultrasound mechanical waves that generate an asymmetric pressure gradient due to the concave geometry of one end of the wire. Recent efforts by Mallouk[13,14] and Wang[15,16] and co-workers have illustrated the possibility of using ultrasound for propelling gold nanowire motors in biologically relevant environments. However, due to their limited surface area, such nanowire motors can only incorporate small quantities of drug payloads.

Dr. V. Garcia-Gradilla, Dr. S. Sattayasamitsathit, F. Soto, Prof. F. Kuralay, Prof. C. Yardımcı, D. Wiitala, M. Galarnyk, Prof. J. Wang
Department of Nanoengineering
University of California
San Diego, La Jolla, CA 92093, USA
E-mail: josephwang@ucsd.edu

DOI: 10.1002/smll.201401013

NANO MICRO small

The present work introduces porous-gold ultrasound nanowire motors with high surface area and tunable porosity towards high efficiency drug loading and release. Porous structures have played a major role in the pharmaceutical industry.[17] Such large surface area structures have been widely used for drug delivery systems[18] but not in connection to the movement of nanomotor carriers. The new ultrasound-powered drug-delivering motors, described in the present work, are based on the incorporation of a nanoporous gold segment into the nanowire structure. Nanoporous gold structures have received considerable attention due to their attractive catalytic, plasmonic and thermal-conductivity properties.[19–25] However, such porous gold materials have not been used in connection to artificial nanomotors or drug delivery system. In contrast, other gold nanostructures have been widely used for drug delivery applications.[26]

Nanoporous gold structures are commonly prepared on two-dimensional flat substrates through electrodeposition of a single-phase Au–Ag alloy followed by etching of the less noble silver component.[19–21] Template-prepared porous nanowires have also been reported,[22–25] but not in connection to nanomotors. The well-controlled template fabrication of the new porous nanomotors allows tuning of their porosity for optimal drug encapsulation. Nanoporous gold nanowires display absorption in the near-infrared (NIR) region[24] that leads to favorable photothermal effects, and can be exploited for an on-demand light-controlled release of the loaded drug. In the following sections, we will characterize the drug encapsulation onto the high-surface area of porous ultrasound nanowire motors and will illustrate that such nanomotors can facilitate the effective loading, guided transport and NIR-triggered release of high therapeutic payloads towards cancer cells (**Figure 1**).

2. Results and Discussion

SEM images of conventional and ultrasound-propelled nanoporous Au nanowire motors are displayed in **Figure 2**. The length of both nanowire motors are 1.8 μm. The nanoporous

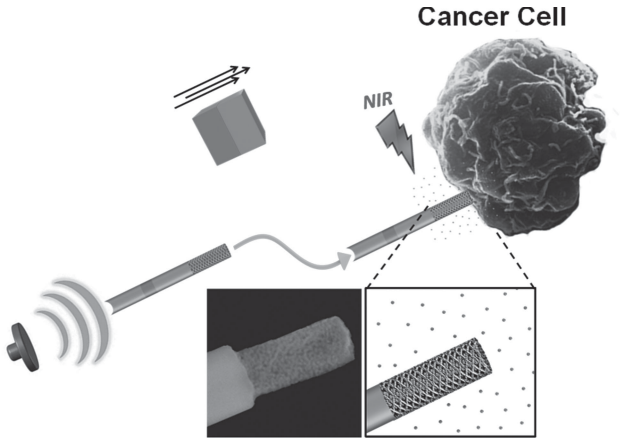

Figure 1. Schematic of the ultrasound-driven movement of the drug-loaded nanoporous Au nanomotors and triggered drug release around a cancer cell.

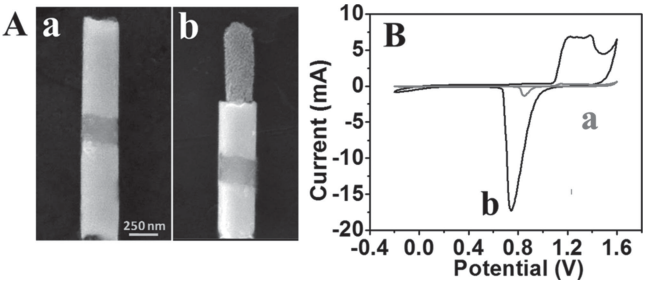

Figure 2. SEM images of different ultrasound nanomotors A): Au/Ni/Au (a), Au/Ni/Au/PAu (b) nanowires. B) Cyclic voltammograms of Au/Ni/Au (a) and Au/Ni/Au/PAu (b) nanowires in N_2-saturated 0.1 M H_2SO_4 using a scan rate of 50 mV s^{-1}.

Au nanowire motors composed of four segments, including solid Au, Ni, Au segments as well as a porous Au one, with the lengths of 0.45, 0.2, 0.45, and 0.63 μm, respectively (Figure 2Ab). The nanoporous Au (PAu) segment has been prepared by plating first an alloy segment by codeposition of Au and Ag at –1.1 V, using a Au/Ag mixture plating solution with a ratio of 7/3 and a charge of 0.2 C. Dealloying the alloy segment (removing the Ag content) was accomplished via a 10 min etching in a 35% HNO_3 solution. This resulted in a nanoporous Au structure with pore sizes of 4–8 nm and ligament diameters of 12–32 nm. The SEM images of Figure 2A indicate a slightly reduced diameter of the nanoporous Au segment, from 280 ± 40 nm (for solid Au) to 250 ± 20 nm (of porous Au). Such decrease in the wire diameter upon the dissolution of the less noble silver reflects the void space formed between the nanowire and the wall of the membrane micropore when free gold atoms (released during the silver etching) diffuse toward the gold-rich center.[22,23,25] Common ultrasound-driven Au/Ni/Au nanowire motors, without the porous Au segment, used as controls, were prepared in a similar manner, but with an extended length of the Au segments (0.8 μm) to obtain the same length as the Au/Ni/Au/PAu nanomotors (Figure 2Aa). The introduction of the nanoporous gold segment has a minimal effect upon the propulsion behaviour of the new motors. Such Au/Ni/Au/PAu nanomotors displayed a speed of around 60 μm/s, that is, over 30 body-lengths per second (using ultrasound power and frequency of 6 V and 2.01 MHz, respectively). Such speed is only 20% lower than that observed for the common solid Au/Ni/Au nanowires (Supporting Information Video 1). The reduced speed can be attributed to the change of the asymmetry and pressure gradient associated with the porous structure.

Cyclic voltammetry (CV) was used to characterize and compare the electrochemically active surface area (ECSA) of the ultrasound Au/Ni/Au/PAu and Au/Ni/Au nanowire motors confined on a glassy carbon electrode (GCE) (Figure 2B). Ultrasound motors released from the membrane template and dispersed in water, were dropped cast onto the GCE, and covered with 5 μL of 0.05% Nafion droplet to secure their confinement. The ECSA measurements were performed in a N_2 saturated 0.1 M H_2SO_4 solution by scanning the potential over the 0.2 to 1.5 V (vs Ag/AgCl) at a scan rate of 50 mV s^{-1}. The ECSA was calculated by integrating the charge associated with the reduction of the oxide

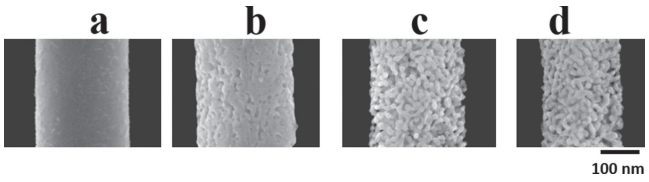

Figure 3. SEM images of a) smooth Au nanowire and nanoporous Au nanowires at different Au/Ag ratios: b) 8:2, c) 7:3, and d) 6:4.

monolayer on the gold surface using GPES software and the reference value of 390 μC cm^{-2} for the Au oxide reduction.[27] The resulting ECSA values for Au and nanoporous Au nanowires are 7.5 and 134 cm^2 (estimated for a batch of wires prepared from a single membrane template). These values indicate that the nanoporous Au structure results in a nearly 20 fold larger surface area compared to the solid gold nanowires. As will be illustrated below, such high specific surface area leads to the loading of greatly larger drug payloads. The controlled fabrication scheme, particularly the composition of the plating solution, allows tuning of the nanoporosity and surface area of the new nanomotors. Different nanoporous morphologies have thus been investigated by systematically changing the gold-to-silver (Au/Ag) ratio in the plating solution from 6/4 to 8/2, while using a deposition potential and dealloying time of –1.1 V and 10 min, respectively. **Figure 3** displays SEM images of solid Au wires (a) and porous Au nanowires (b,d) prepared from the different plating solution mixtures. The gold-rich plating solution, with a Au/Ag ratio of 8/2 (b), leads to a nearly solid and rough surface, with negligible porosity, reflecting the low silver content of the alloy. In contrast, increasing the silver content, using plating solutions with Au/Ag ratios of 7/3 (c) and 6/4 (d), results in increased nanoporosity and smaller wire diameters of 250 ± 20 nm and 230 ± 20 nm, respectively. Closer examination of these images indicate that the porous gold nanowire, prepared from a plating solution with a Au/Ag ratio of 7/3 offer the largest surface area.

Figure 4 displays the DOX loading capacity (a) and release behaviour (b) using the nanoporous and solid gold nanowires modified with three different coatings (essential for confining the DOX): negatively charged poly(sodium 4-styrenesulfonate) (PSS) or poly(acrylic) acid (PAA) and a methyl thioglycolate (MTG) "agent". The polyelectrolytes were coated onto the nanomotor surface by immersing a batch of the nanomotors (from a single membrane template) into 1 mL of the PSS or PAA solutions (2 mg/mL polyelectrolyte in 6 mM NaCl) for 3 h followed by washing three times with water. The conjugation between PSS and DOX proceeds not only via electrostatic interaction between the negatively-charged sulfonate group of PSS and positively-charged amine group of DOX, but may involve additional hydrogen bonding between the amino and hydroxyl groups of DOX and the sulfonate group of PSS.[28] Similarly, electrostatic interactions have been used for attaching the cationic DOX to the anionic PAA films.[29] A batch of coated nanomotors, prepared from a single membrane template, was added to one mL of 0.1 mM DOX (prepared in 25 mM MES buffer pH 6.5). The reaction proceeded overnight under dark conditions. The loading amount of DOX onto the nanomotors was quantified by measuring UV absorption of the DOX solution before and after such incubation. Ultrasound nanomotors, prepared from a single membrane template were dried and weighed and were used for calculating (and normalizing) the loading capacity per weight of nanomotors. The DOX loading capacity onto the solid nanomotors was normalized to the same length as of the porous segment. The PSS-modified porous Au nanomotors yielded the highest DOX loading capacity of 17.9 μg/membrane, corresponding to 13.4 μg/mg nanomotors (Figure 4Aa). PAA-modified porous Au nanomotors yielded a slightly lower loading capacity of 16.9 μg/membrane or 12.6 μg/mg nanomotor (Figure 4Ba). In contrast, DOX conjugated to the MTG-modified nanoporous gold surface via a hydrazine linker,[30] resulted in the lowest loading capacity of 11.5 μg/membrane or 8.6 μg/mg nanomotor (Figure 4Ca). The modification of the motor with the thiolated MTG is described in detail in the Supporting Information. The PSS-modified porous gold nanomotors also displayed an 8-fold higher loading capacity compared to the solid gold nanowires, reflecting their greatly larger surface area.

The drug release from the ultrasound nanowire motors was carried out at room temperature by irradiation of the samples using NIR (808 nm for 15 min) in a PBS buffer solution (pH 7.4). The supernatants were analyzed using UV–Vis spectroscopy. Due to localized surface plasmon resonance and photothermal effects of nanoporous gold when considering as clusters of small nanoparticles and interconnected ligaments,[24,31] the conversion of absorbed light energy as heat can induce local structural changes of the anionic polymer and lead to effective release of the payload.[32–34] To reduce the exposure time and intensity of the NIR radiation, nanowire motors can be further tailored by controlling their aspect ratio (both diameter and length), as well as adjusting their nanoporosity, as desired for minimizing the light effect upon the tissues and physiological fluids. The data of Figure 4Ab suggest that the PSS-modified nanoporous gold can release 5.5 μg DOX per mg of nanomotor, or up to ≈40%

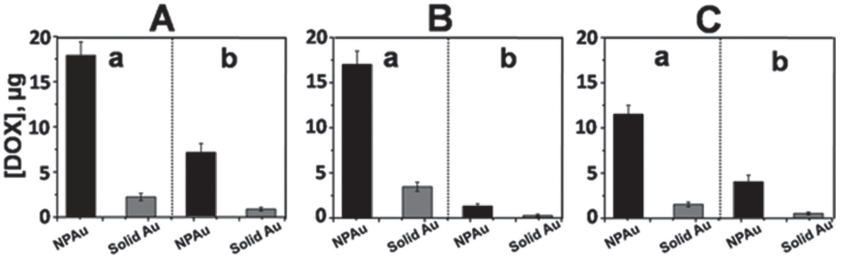

Figure 4. a) Loading capacity and b) NIR-triggered release of DOX from solid Au (grey) and nanoporous Au (black) nanowires based on different coatings prepared from: A) 2 mg/mL PSS, B) 2 mg/mL PAA, C)10 mM MTG. The DOX loading was calculated for a batch of nanomotors prepared from one membrane template. See details and related calculations in the experimental and discussion sections. DOX releasing conditions: 15 min NIR light irradiation (808 nm, 4 W/cm^2) in a PBS buffer pH 7.4. The DOX loading capacity of the solid nanowire motors was normalized to the same length of the nanoporous segment.

NANO MICRO small

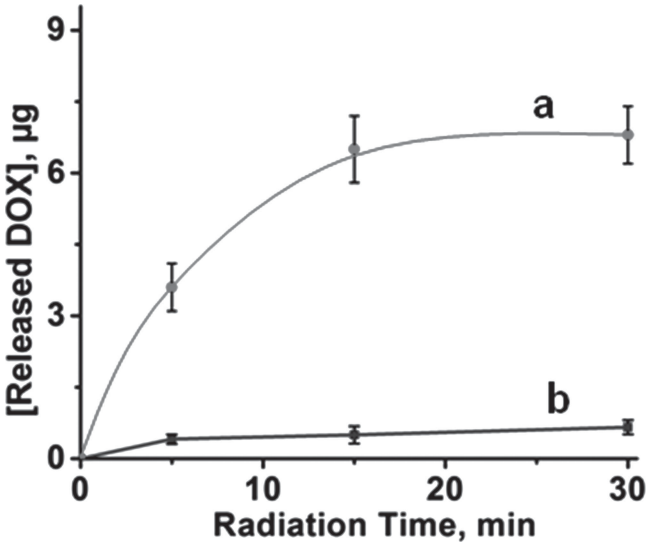

Figure 5. NIR-triggered anticancer drug DOX release with a function of irradiation time using a) PSS modified PAu nanomotors and b) Au nanomotors. The amount of released DOX was calculated for a batch of nanomotors prepared from one membrane template. Release conditions: NIR laser wavelength 808 nm and power of 4 W/cm^2 was used. The drug release was carried out in PBS buffer (pH 7.4). The % release of DOX from the Au nanomotors was normalized to the same length of the porous segment.

of their drug payload using such NIR light (Figure 4Ab). In contrast, the PAA-modified nanoporous gold nanowires can release only 1.0 μg/mg nanomotor, or up to 7.9% of the loaded DOX (Figure 4Bb). The lower DOX release capability of the PAA-modified nanoporous gold can be attributed to the stronger electrostatic interaction between the charged polymer and DOX. The MTG-modified nanomotors can release 3.7 μg/mg nanomotor or 43.6% release of the loaded drug (Figure 4Cb). These results of Figure 4 confirm that light-controlled release of the drug can be achieved through photothermal effects mediated by the nanoporous Au structure.

Subsequently, we examined the NIR-triggered release of DOX from PSS-modified PAu nanomotors as a function of the irradiation time. **Figure 5**a displays the drug release profile upon increasing the irradiation time (for a batch of nanomotors prepared from a single membrane template). A one stage profile is observed with a fast initial release rate followed by a slower release. These data suggest that nearly 6.8 μg, or ≈38% of the payload, can be released during a 15 min irradiation using the 808 nm NIR light (4 W/cm^2), considering that the loading amount of DOX on the PSS-modified nanoporous Au nanomotors (from one membrane) is 17.9 μg. No improvement in the DOX release efficiency is observed upon extending the irradiation time to 30 min. A control experiment, using the DOX-loaded PSS-modified nanoporous gold but without the NIR irradiation, was also carried out at room temperature. The results suggest that only 0.9 μg DOX, or ≈5% of the loaded drug, was released (not shown). Another control experiment was carried out using the PSS-modified non-porous Au nanomotors (Figure 5b). Only a small amount of DOX (≈0.6 μg) was released over the 30 min long NIR irradiation time, a substantially (>10) lower level compared to the nanoporous Au nanowires (a vs b). The loading amount of DOX on the PSS-modified non-porous nanomotors (from a single membrane) is 2.5 μg.

The ability of the drug-loaded ultrasound-powered porous nanomotors to approach a cancer cell and release the therapeutic payload on demand is demonstrated in **Figure 6** and Supporting Information Video 2. These data illustrate the DOX-loaded nanoporous vehicles traveling towards the HeLa cell (A), approaching the targeted cell (B), and finally releasing the drug (via NIR irradiation) around the cell (C). The release of DOX from nanoporous gold segment or gold nanorods was monitored using fluorescence optical imaging, based on the intrinsic fluorescence properties of DOX. A fixed HeLa cell, with autofluorescence properties, was used here. The drug, as well as the HeLa cell, can thus be visualized under fluorescence microscope. The effect of NIR laser exposure on the drug release was thus investigated using the changes in the fluorescent intensity before and after exposure to the light. Arrival of the nanomotor to the cell is indicated from the high fluorescent intensity of the encapsulated DOX (B). A significant quenching of the fluorescence on the nanowire surface is observed following a 15 min of NIR laser irradiation (1 W/cm^2, 808 nm), reflecting the release of the drug (C). No such changes in the fluorescence intensity were observed in a control experiment carried out without the NIR irradiation (not shown). Generally, using NIR-light in connection to nanoporous Au structures increase the temperature from ≈20 to ≈40 °C within 1 min,[31] which would have a minor effect upon loading drug. The heat associated with DOX release also showed the synergistic effect upon deconstruction of the tumor cells.[35,36]

3. Conclusions

In conclusion, we demonstrated that nanoporous gold nanowire motors offer efficient drug loading, transport and release capabilities. Template deposition has been shown extremely useful for tailoring nanoporosity and maximizing the available surface area of the nanowire motor for efficient drug loading. Additional improvements in the drug loading capacity are expected by coupling the new nanoporous motor surface with in connection to layer-by-layer loading. The photothermal effects of the nanoporous gold have been exploited for an on-demand drug release via a NIR irradiation. Such ultrasound-powered nanomotors offer

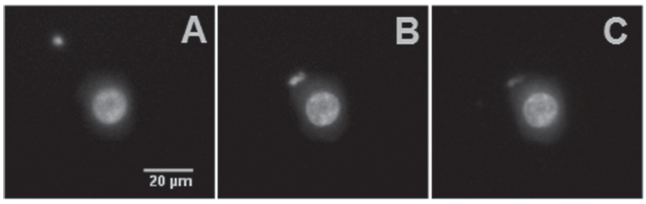

Figure 6. Time-lapse fluorescent images of the DOX-loaded NPAu nanomotor A) travelling towards a HeLa cell, B) approaching the HeLa cell, and of C) the nanomotor and the HeLa cell after 15 min of NIR irradiation. DOX release conditions, as in Figure 4. Motion of NPAu nanomotors was achieved under ultrasound propulsion at 6 V and 2.01 MHz.

a potentially extremely attractive approach for rapidly delivering larger therapeutic payloads to predetermined destinations in a target specific manner, and could be extended to different applications, such as gene delivery. Improved specificity could be achieved by the incorporation of appropriate ligands. As future US-driven nanomachines become more functional, these tiny devices are expected to perform more diverse and important biomedical applications, facilitating tailored and personalized disease treatment.

4. Experimental Section

Materials and Instruments: Anodisc alumina membranes (AAO) with a specified pore size of 200 nm and thickness of 60 μm were purchased from Whatman (Catalog No. 6809–6022; Maidstone, UK). The gold and silver plating solutions (Orotemp 24 RTU RACK, and 1025 RTU @ 4.5 Troy/gallon) were obtained from Technic Inc. (Anaheim, CA). Poly(sodium 4-styrenesulfonate), brilliant green and DOX hydrochloride were purchased from Sigma-Aldrich (St. Louis, MO, USA). Sodium chloride was obtained from Fisher Scientific (Fair Lawn, New Jersey, USA). All chemicals were analytical-grade reagents and were used as received without any further purification and prepared by dilution in deionized water otherwise specified. Experiments were carried out at room temperature (21 °C). All controlled-potential experiments were performed with a CHI 621A potentiostat (CH Instruments, Austin, TX). The ECSA characterization was carried out using a μ-Autolab type II (Eco Chemie, Utrecht, Netherlands), operating with GPES software, and a conventional three-electrode electrochemical cell.

Synthesis of the Drug Delivery Porous Nanomotors: The nanowire motors were prepared by a template-directed electrodeposition method using AAO membranes as a template. A silver film was sputtered on branched side of the AAO membrane template to serve as a working electrode. The membrane was then assembled in a plating cell with aluminum foil serving as a contact. A sacrificial silver layer was electrodeposited for a total charge of 3 C using a commercial silver plating solution at a potential of −1.0 V (vs Ag/AgCl (1 M KCl)), in connection with a Pt wire counter electrode. Subsequently, a Au segment was electroplated at a potential of −1.0 V for a total charge of 0.8 C using a commercial plating solution. Nickel was deposited from a nickel plating solution containing $NiCl_2{\cdot}6H_2O$ (20 g L^{-1}), $Ni(H_2NSO_3)_2{\cdot}4H_2O$ (515 g L^{-1}), and H_3BO_3 (20 g L^{-1}) at −1.0 V for 1 C. Next, another Au segment was electroplated at a potential of −1.0 V for a total charge of 0.8 C. Finally, a nanoporous Au segment was prepared from a mixture of commercial gold and silver plating solutions, using different Au/Ag ratios (ranging from 6/4 to 8/2), at a potential of −1.1 V for 0.5 C. The Au/Ag alloy segment was dealloyed using a 35% HNO_3 solution (EMD Millipore, MA) for 10 min. This protocol leads to Au/Ni/Au/NPAu nanowires embedded in the membrane template. The membranes were then removed from the growth cell and rinsed thoroughly with nanopure water. The sacrificial silver layer was removed using a cotton tip applicator soaked in 35% HNO_3 solution. The AAO membrane template was dissolved in a 3 M NaOH solution for 30 min to release the nanowires motors. The nanowires were collected using a magnetic field and were washed repeatedly with deionized water until a neutral pH was achieved. Control non-porous Au/Ni/Au nanowire motors were prepared in the same manner as mentioned above, except both Au segments were electroplated for 1.2 C.

Surface Modification using Poly(sodium 4-styrenesulfonate) or Poly(acrylic acid) Layers: The poly(sodium 4-styrenesulfonate) (PSS) layer or Poly(acrylic acid) (PAA) was coated on the nanoporous Au and Au nanomotors by incubating a batch of nanomotors prepared from a single membrane in 1 mL of 2 mg/mL PSS or PAA solution containing 1 mM NaCl for 3 h. After incubation the Au nanostructures were washed with nanopure water (18.2 MΩ cm) to remove excess polymer. Next, the conjugation of DOX on the PSS or PAA films was carried out by incubating the 1.34 mg of the polyelectrolyte-coated nanomotors (from one membrane preparation) in a 1 mL solution containing 0.1 mM DOX overnight via electrostatic interaction.[29] The drug conjugated nanoporous or solid gold nanowires were then washed with nanopure water to remove all unconjugated drug molecules by centrifugation at 6000 rpm for 5 min. The drug-conjugated nanomotors were then added to PBS buffer solutions (pH 7.4) to test the drug release capability.

Modification of Methyl thioglycolate (MTG) Layer on NPAu Nanomotors: The methyl thioglycolate (MTG) layer was coated on a nanoporous Au nanomotors and Au nanomotors by incubating free nanomotors after dissolving the membrane (prepared from one AAO membrane) into 1 mL of 10 mM MTG in 10% methanol. The mixture was allowed to react in the dark for 24 h to form stable thiol monolayers on the gold surface. Thiol-stabilized nanoporous Au segment or Au nanowires were subjected to a reaction with hydrazine. Hydrazine (1 mM) was added to thiol-stabilized nanoporous Au segment or Au nanomotors under continuous stirring at 50 °C for 24 h. Subsequently, the Au nanomotors were washed with nanopure water (18.2 MΩ cm) and DOX was covalently attached to the surface by a reaction between the hydrazine moiety of the MTG domain and the ketonic groups of DOX.

Ultrasound Propulsion: The ultrasonic experiments were carried out in a cell similar to that described previously.[14,16] The cell was made in a glass slide 75 mm × 25 mm × 1 mm (instead of a metallic plate for enhancement of fluorescence experiments), covered by PDMS template 10 mm × 10 mm × 0.25 mm with a center hole of 5 mm in diameter as the sample reservoir, covered by a 18 mm × 18 mm × 0.15 mm cover slide for reflection of the ultrasound waves and for stability of the solution (to avoid motion of the solution due to disturbances of the environment). The piezoelectric unfocused ultrasonic transducer which produces the ultrasound waves (Physik Instrumente PZT ring 0.5 mm thickness, 10 mm outside diameter by 5 mm center-hole diameter) was attached to the bottom center of the glass slide. The continuous ultrasound sine wave was applied via a piezoelectric transducer, through an Agilent 15 MHz arbitrary waveform generator, in connection to a home-made power amplifier. The applied sine wave had a frequency of 2.01 MHz. The voltage amplitude (Vpp) of 6 V, correspond to a maximum power density of 0.383 W/cm^2, respectively, as needed for controlling the intensity of the ultrasonic wave (considering the power is distributed only in the transducer area). The electric signal was monitored using a 20 MHz Tektronix 434 storage oscilloscope. The motion of the nanomotors was visualized using a Nikon Eclipse 80i upright microscope. The fluorescence images and videos of DOX-loaded nanomotors were captured using a B-2A (C72181) FITC filter. All videos were taken with a 20× objective and acquired at 5 frames/s with a PhotometricsCoolSnap HQ2 1392 × 1040 pixels CCD camera, attached to the microscope,

and were processed with Metamorph 7.7.5 software (Molecular Devices, Sunnyvale, CA).

Near-Infrared Light-triggered Drug Release from the Nanomotors: The drug release of DOX from the different coated nanoporous and solid Au nanowires were performed in a similar manner. The DOX-loaded nanowires were repeatedly washed with DI water to remove unconjugated drug and resuspended in PBS buffer pH 7.4 to emulate physiological conditions. Triggered drug release was performed by photothermal process by NIR radiation (808 nm, 4 W/cm^2) using different irradiation times (0, 5, 15, 30 min). The released drug was estimated by analyzing the solution using UV-VIS spectroscopy based on the DOX absorbance at 480 nm. For dynamic drug release of DOX, drug loaded nanomotors were first washed and centrifuged 4 times with DI water to remove unconjugated drug, and finally re-suspended in 1 mL of PBS buffer (pH 7.4). A 2.5 µL aliquot of the nanomotors is then placed into transparent setup reservoir and covered with a cover slide. The nanomotors were ultrasound propelled and magnetically guided towards the HeLa cancer cell target and NIR-triggered drug release was achieved by irradiating the nanomotors with an 808 nm wavelength, 200 mW laser beam for 5 min intervals. Fluorescent images were taken at every radiation interval using UV filter to observe the release of DOX from the nanomotors.

Supporting Information

Supporting Information is available from the Wiley Online Library or from the author.

Acknowledgements

V.G-G., S.S., and F.S. contributed equally to this work. This project received support from the Defense Threat Reduction Agency-Joint Science and Technology Office for Chemical and Biological Defense (Grant no. HDTRA1–13–1–0002). V.G., F.K. and C.Y. acknowledge financial support from Centro de Nanociencias y Nanotecnología UNAM (Mexico), the Interdisciplinary Council of Turkey (YOK), and the Scientific and Technological Research Council of Turkey (TUBITAK), respectively. The authors thank Ernesto Magaña for his assistance.

[1] J. Wang, *Nanomachines: Fundamentals and Applications* Wiley-VCH, Weinheim, Germany **2013**, ISBN 978–3–527–33120–8.
[2] T. Mirkovic, N. S. Zacharia, G. D. Scholes, G. A. Ozin, *ACS Nano* **2010**, *4*, 1782.
[3] L. K. E. A. Abdelmohsen, F. Peng, Y. Tu, D. A. Wilson, *J. Mater. Chem. B* **2014**, *2*, 2395.
[4] S. Sengupta, M. E. Ibele, A. Sen, *Angew. Chem. Int. Ed.* **2012**, *51*, 8434.
[5] K. E. Peyer, L. Zhang, B. J. Nelson, *Nanoscale* **2013**, *5*, 1259.
[6] J. Wang, W. Gao, *ACS Nano* **2012**, *6*, 5745.
[7] D. Kagan, R. Laocharoensuk, M. Zimmerman, C. Clawson, S. Balasubramanian, D. Kang, D. Bishop, S. Sattayasamitsathit, L. Zhang, J. Wang, *Small* **2010**, *6*, 2741.
[8] Z. Wu, Y. Wu, W. He, X. Lin, J. Sun, Q. He, *Angew. Chem. Int. Ed.* **2013**, *52*, 7000.
[9] W. Gao, D. Kagan, O. S. Pak, C. Clawson, S. Campuzano, E. C. Erdene, E. Shipton, E. E. Fullerton, L. Zhang, E. Lauga, J. Wang, *Small* **2012**, *8*, 460.
[10] B. J. Nelson, I. K. Kaliakatsos, J. J. Abbott, *Annu. Rev. Biomed. Eng.* **2010**, *12*, 55.
[11] M. Suter, L. Zhang, E. C. Siringil, C. Peters, T. Luehmann, O. Ergeneman, K. E. Peyer, B. J. Nelson, C. Hierold, *Biomed. Microdevices* **2013**, *15*, 997.
[12] F. Qiu, R. Mhanna, L. Zhang, Y. Ding, S. Fujita, B. J. Nelson, *Sens. Actuators B: Chem.* **2014**, *196*, 676.
[13] W. Wang, L. A. Castro, M. Hoyos, T. E. Mallouk, *ACS Nano* **2012**, *6*, 6122.
[14] W. Wang, S. Li, L. Mair, S. Ahmed, T. J. Huang, T. E. Mallouk, *Angew. Chem. Int. Ed.* **2014**, *53*, 3201.
[15] D. Kagan, M. J. Benchimol, J. C. Claussen, E. C. Erdene, S. Esener, J. Wang, *Angew. Chem.* **2012**, *124*, 7637.
[16] V. Garcia-Gradilla, J. Orozco, S. Sattayasamitsathit, F. Soto, F. Kuralay, A. Pourazary, A. Katzenberg, W. Gao, Y. Shen, J. Wang, *ACS Nano* **2013**, *7*, 9232.
[17] Z.-Z. Li, L.-X. Wen, L. Shao, J.-F. Chen, *J. Controlled Release* **2004**, *98*, 245.
[18] F. Tang, L. Li, D. Chen, *Adv. Mater.* **2012**, *24*, 1504.
[19] J. Erlebacher, M. J. Aziz, A. , Karma, N. Dimitrov, K. Sleradzki, *Nature* **2001**, *410*, 450.
[20] A. Wittstock, V. Zielasek, J. Biener, C. M. Friend, M. Bäumer, *Science* **2010**, *327*, 319.
[21] C. Xu, J. Su, X. Xu, P. Liu, H. Zhao, F. Tian, Y. Ding, *J. Am. Chem. Soc.* **2007**, *129*, 42.
[22] C. Ji, P. C. Searson, *J. Phys. Chem. B* **2003**, *107*, 4494.
[23] C. Ji, P. C. Searson, *Appl. Phys. Lett.* **2002**, *81*, 4437.
[24] H.-M. Bok, K. L. Shuford, S. Kim, S. K. Kim, S. Park, *Nano Letters* **2008**, *8*, 2265.
[25] S. Sattayasamitsathit, Y. Gu, K. Kaufmann, S. Minteer, R. Polsky, J. Wang, *Nanoscale* **2013**, *5*, 7849.
[26] P. Ghosh, G. Han, M. De, C. K. Kim, V. M. Rotello, *Adv. Drug Delivery Rev.* **2008**, *60*, 1307.
[27] S. Trasatti, O. A. Petrii, *J. Electroanal. Chem.* **1992**, *327*, 353.
[28] R. Venkatesan, A. Pichaimani, K. Hari, P. K. Balasubramanian, J. Kulandaivel, K. Premkumar, *J. Mater. Chem. B* **2013**, *1*, 1010.
[29] T. Wang, X. Zhang, Y. Pan, X. Miao, Z. Su, C. Wang, X. Li, *Dalton Trans.* **2011**, *40*, 9789.
[30] S. Aryal, J. J. Grailer, S. Pilla, D. A. Steeberb, S. Gong, *J. Mater. Chem.* **2009**, *19*, 7879.
[31] G. M. Santos, F. Zhao, J. Zeng, W.-C. Shih, *Nanoscale* **2014**, *6*, 5718.
[32] B. P. Timko, T. Dvir, D. S. Kohane, *Adv. Mater.* **2010**, *22*, 4925.
[33] R. Huschka, A. Barhoumi, Q. Liu, J. A. Roth, L. Ji, N. J. Halas, *ACS Nano* **2012**, *6*, 7581.
[34] B. G. De Geest, N. N. Sanders, G. B. Sukhorukov, J. Demeestera, S. C. De Smedt, *Chem. Soc. Rev.* **2007**, *36*, 636.
[35] S.-M. Lee, H. Park, K.-H. Yoo, *Adv. Mater.* **2010**, *22*, 4049.
[36] F. Gao, L. Li, T. Liu, N. Hao, H. Liu, L. Tan, H. Li, X. Huang, B. Peng, C. Yan, L. Yang, X. Wu, D. Chen, F. Tang, *Nanoscale* **2012**, *4*, 3365.

Received: April 11, 2014
Revised: June 6, 2014
Published online: July 3, 2014

